Lofts, Stephen; Tipping, Edward; Lawlor, Alan J.; Shotbolt, Laura. 2013. **An intermediate complexity dynamic model for predicting accumulation of atmospherically-deposited metals (Ni, Cu, Zn, Cd, Pb) in catchment soils: 1400 to present.**

Contact CEH NORA team at
noraceh@ceh.ac.uk

1

An intermediate complexity dynamic model for predicting accumulation of atmospherically–deposited metals (Ni, Cu, Zn, Cd, Pb) in catchment soils: 1400 to present

5

6   Stephen LOFTS[a,*], Edward TIPPING[a], Alan LAWLOR[a], Laura SHOTBOLT[b]

7

8   [a] NERC Centre for Ecology and Hydrology, Lancaster Environment Centre, Bailrigg,
9   Lancaster, LA1 4AP, United Kingdom. emails: stlo@ceh.ac.uk, et@ceh.ac.uk,
10 ajlaw@ceh.ac.uk

11 [b] School of Geography, Queen Mary, University of London, Mile End Road, London E1
12 4NS, United Kingdom. Email: l.shotbolt@qmul.ac.uk

13 * Corresponding author. E-mail: stlo@ceh.ac.uk

14

Abstract

16 The Intermediate Dynamic Model for Metals (IDMM) is a model for prediction of the pools
17 of metals (Ni, Cu, Zn, Cd, Pb) in topsoils of catchments resulting from deposition of metals
18 from the atmosphere. We used the model to simulate soil metal pools from 1500 onwards in
19 ten UK catchments comprising semi-natural habitats, and compared the results with present
20 day observations of soil metal pools. Generally the model performed well in simulating
21 present day pools, and further improvements were made to simulations of Ni, Cu, Zn and Cd
22 by adjusting the strength of metal adsorption to the soils. Some discrepancies between
23 observation and prediction for Pb appeared to be due either to underestimation of cumulative
24 deposition, or to overestimation of the metal pool under 'pristine', pre-industrial conditions.
25 The IDMM provides a potential basis for large scale assessment of metal dynamics in
26 topsoils.

Keywords

28 Metals; soils; dynamic modelling; atmospheric deposition

29   *Capsule*

30   The Intermediate Dynamic Model for Metals predicts the present day pools of Ni, Cu, Zn, Cd

31   and Pb in semi–natural catchment soils of the UK.

32   **1.   Introduction**

33   Soils may become contaminated by metals from a variety of sources including mining and

34   smelting activities, atmospheric deposition and land application of materials such as manures

35   and sludges. Since metals tend to associate strongly with soil solids, responses of soil

36   concentrations to changes in inputs, particularly decreases, are predicted to occur on

37   timescales from decades to centuries (Paces, 1998). Thus, current concentrations of metals in

38   soils, and leaching to groundwater and surface waters, are highly dependent upon historic

39   inputs. The critical loads approach (e.g. Hall et al., 2006; Lofts et al., 2007; de Vries and

40   Groenenberg, 2009) uses the steady state concept as a starting point for assessing the

41   sensitivity of soils to metal contamination. It is clear, however, that the timescales of metal

42   accumulation and leaching in soils are sufficiently slow to warrant dynamic modelling for

43   more realistic assessment of future risks.

44   Approaches for long term (decades or longer) dynamic modelling of metals in soils vary in

45   sophistication and range of applicability, from detailed catchment models such as the

46   Chemistry of the Uplands Model (CHUM; CHUM–AM) (Tipping, 1996; Tipping et al.,

47   2006a; Tipping et al., 2006b) and the SMARTml model (Bonten et al., 2011) to simpler

48   models such as those presented by Posch and de Vries (2009) and de Vries and Groenenberg

49   (2009) or the TRANSPEC–II model of Bhavsar et al. (2008). The CHUM model simulates

50   the long-term chemistry of both major ions and metals, taking into account solid-solution

51   partitioning of major ions (Na, Mg, Al, K, Ca) and trace metals, mineral weathering, and

52   cycling of C, N and S in soils. Thus, CHUM–AM can simulate mechanistically the

53   confounding effects of changes in soil pH status and C cycling on metal accumulation and

54   release over time. The dynamic models presented by Posch and de Vries (2009) and de Vries

55   and Groenenberg (2009) are intended for the calculation of target loads of input metal over a

56   defined period. Transfers between metal pools (e.g. soil-bound and dissolved) are calculated

57   using a combination of empirical and mechanistic modelling, while potential confounding

58   effects such as changes in porewater pH or dissolved organic carbon (DOC) in drainage water

59   are not simulated. Complex models such as CHUM–AM are applicable for catchments where

60   detailed monitoring data are available for parameterisation and testing, while the simpler

2

61 models are more suitable for larger scale application where less detailed data are available for
62 parameterisation.

63 In this paper we present a dynamic model for metals in soils that is intermediate in
64 complexity between CHUM–AM and the simpler dynamic models. The Intermediate
65 Dynamic Model for Metals (IDMM) combines mechanistic and empirical submodels to
66 describe metal speciation in the soil and runoff, within a flexible framework whereby
67 temporal changes in driving variables such as metal deposition, porewater pH and DOC may
68 be imposed. We describe the model structure, inputs and limitations, and demonstrate its
69 application to prediction of historical metal accumulation in a set of UK catchments
70 comprising semi-natural habitats. The objective is to demonstrate the utility of the IDMM as
71 a tool for predicting present day and future metal concentrations in soils as a result of past,
72 current and future metal inputs.

73 **2.   Materials and methods**

74 *2.1.   Intermediate Dynamic Model for Metals*

75 The IDMM simulates a single chemically and physically homogenous soil layer, composed
76 of fine soil (comprising material <2mm), stones (inorganic material > 2mm) and pore space,
77 which represents an idealised average composition of the catchment soil. The pore space is
78 occupied by air and water. The depth of soil to be simulated is the choice of the user. In this
79 study we have simulated complete soil profiles, to bedrock, for the non-peat soils. In peat
80 soils the acrotelm only was simulated. The relative proportions of fine soil, stones, water and
81 unoccupied pore space making up the soil layer are assumed not to change over time. The
82 soil layer is defined by its depth (m), bulk density (g m^{-3}), organic matter content (%) (SOM),
83 the proportion of the total volume that is occupied by stones (%), the proportion of the
84 catchment that is bare rock (%), and the soil water content (% saturation of the pore space).
85 The density of the fine soil is calculated by assuming the soil mineral matter to have a
86 particle density of 2.6×10^6 g m^{-3} and the soil organic matter to have a density of 1.5×10^6
87 g m^{-3}. These variables are used to calculate the concentration of fine soil (g soil per m^3
88 porewater) in the soil layer.

89 *Metal fluxes and mass balance*

90 The model runs on an annual timestep. Metal (Ni, Cu, Zn, Cd, Pb) may be either adsorbed to
91 the fine soil solids, dissolved in the porewater, or adsorbed to eroded fine soil in the

3

92   porewater. Together, these forms comprise the pool of 'geochemically active' or labile metal.

93   On each timestep, metal enters the soil as an input to the soil surface (e.g. from atmospheric

94   deposition) and by mineral weathering, and is assumed to mix completely with the metal

95   already present. Inputs of metal are assumed to be completely geochemically active. The

96   pool of mineral-associated metal is not explicitly simulated beyond the simulation of

97   weathering inputs to the geochemically active pool over time. The 'fixation' or 'aging' of

98   metal into soil particles is not simulated. Metals are lost from the soil layer by porewater

99   leaching. The mass balance of metal in the soil layer is given by the expression

100    $$\Delta M_{soil} = \frac{F_{input} + F_{weath}}{1 - f_{rock}} - L \cdot 10^3 \left(\{M\}_{ads} \cdot [ES] + [M]_{pw,diss} \right). \tag{1}$$

101   The terms in this equation are as follows:

- 102 ΔM_{soil} is the change in the geochemically active metal pool in the soil in one year, in
- 103   mol per m^2 of soil);
- 104 F_{input} and F_{weath} are the inputs of metal to the soil surface and by mineral weathering,
- 105   respectively, in mol per m^2 of the catchment. The metal input to the soil surface may
- 106   vary over time, while the weathering rate is assumed to be constant;
- 107 f_{rock} is the proportion of the catchment area that is bare rock;
- 108   L is the annual leaching volume of water from the soil layer, in m^3 per m^2 of soil area;
- 109 $\{M\}_{ads}$ is the adsorbed part of the geochemically active metal pool in mol per g of
- 110   fine soil;
- 111   [ES] is the concentration of eroded soil in the porewater in g dm^{-3};
- 112 $[M]_{pw,diss}$ is the concentration of dissolved metal in the porewater.

113   *Soil-porewater partitioning of metal*

114   The model calculates the partitioning of the geochemically active metal between the solid

115   (soil) and solution (porewater) phases using a combination of two submodels. A semi-

116   empirical Freundlich transfer function is used to describe the relationship between the

117   adsorbed pool and the free metal ion in porewater, and the WHAM/Model VI equilibrium

118   speciation model calculates the dissolved metal in porewater from the free ion. The transfer

119   function relates the adsorbed and free ion forms of the metal in the soil layer:

120    $$\log\left(\frac{\{M\}_{ads}}{[M]^{\frac{1}{n}}_{free}} \right) = \alpha_0 + \alpha_1 \cdot pH + \alpha_2 \cdot \log\left(\%SOM\right). \tag{2}$$

4

121   The terms α_0, α_1, α_2 and n are fitted constants, and $\{M\}_{ads}$ and $[M]_{free}$ are the geochemically

122   active metal pool (mol per g fine soil) and the free metal ion in porewater (mol per dm^3),

123   respectively. The %SOM is the % organic matter content of the fine soil.

124   The concentration of metal dissolved in the porewater is calculated from the free ion

125   concentration using WHAM/Model VI. This calculation requires specification of the

126   porewater chemical composition (pH, concentrations of ionic species and dissolved organic

127   carbon (DOC)). The chemical composition of the porewater is determined as follows:

128   •   The pH is a time–variant input;

129   •   the concentrations of sodium and chloride are fixed to 1.00×10^{-3} mol dm^{-3} and

130   3.33×10^{-4} mol dm^{-3} respectively;

131   •   the concentrations of calcium, nitrate and sulphate are initially set to zero, 3.33×10^{-4}

132   mol dm^{-3} and 1.67×10^{-4} mol dm^{-3} respectively. During model initialisation, the

133   concentration of either calcium, or the combined concentrations of nitrate and

134   sulphate, are adjusted to achieve charge balance;

135   •   iron(III) and aluminium are specified by estimation of their free ion activities. The

136   activity of iron(III) is specified by assuming equilibrium with precipitated iron(III)

137   hydroxide (Lofts et al., 2008). The activity of aluminium is specified using the

138   expressions derived by Tipping (2005) for activity in soil solutions. Following

139   Tipping (2005), different expressions are used for 'mineral' soils (having less than

140   20% organic matter) and 'organic' soils (greater than or equal to 20% organic matter);

141   •   the carbonate concentration is calculated assuming it to be in equilibrium with CO_2 in

142   the soil atmosphere. The partial pressure of CO_2 is a fixed input. For the calculations

143   presented here we assumed a partial pressure of CO_2 of 3.8×10^{-3} atm in the soil

144   atmosphere, ten times the pressure in the open atmosphere.

145   •   the DOC concentration is specified as a model input, which may change from year to

146   year. Binding of ions by dissolved organic matter (DOM) is simulated assuming each

147   unit mass of DOM to have binding properties equivalent to 0.65 unit masses of fulvic

148   acid (FA) (i.e. 1 mg dm^{-3} DOM is equivalent to 0.65 mg dm^{-3} of FA). The DOM is

149   assumed to comprise 50% carbon.

150   The concentration of metal adsorbed to eroded fine soil in the porewater is computed from

151   the concentration of eroded fine soil and the concentration of adsorbed metal per unit mass of

fine soil. The concentration of eroded fine soil in the soil porewater is specified as a model
153 input. The mass of fine soil in the soil layer is not corrected for erosion losses.

2.2. Dynamic modelling

155 To simulate metal dynamics in a soil layer, the model is run from a chosen starting year in the
156 past which is assumed to represent pristine conditions with respect to metal inputs, i.e. when
157 inputs are assumed to comprise only atmospheric deposition of metal from natural sources
158 such as volcanism. Furthermore, the soil pool of geochemically active metal is assumed to be
159 in steady state in the starting year, such that losses in leaching balance inputs from deposition
160 and weathering. Under the steady state assumption, $\Delta M_{soil} = 0$, so Equation (1) can be
161 rearranged as follows:

162
$$\frac{F_{input} + F_{weath}}{1 - f_{rock}} = L \cdot 10^3 \left(\{M\}_{ads} \cdot [S] + [M]_{pw,diss} \right)$$

163 and $[M]_{pw,total} = \{M\}_{ads} \cdot [S] + [M]_{pw,diss} = \dfrac{F_{input} + F_{weath}}{\left(1 - f_{rock}\right) L \cdot 10^3}$ (3)

164 where $[M]_{pw,total}$ is the total metal concentration (dissolved and adsorbed to eroded soil) in the
165 porewater. Initially, $[M]_{pw,total}$ is calculated from the pristine metal inputs and runoff, then
166 $[M]_{free}$ and $\{M\}_{ads}$ at steady state are calculated iteratively using the transfer functions and
167 WHAM/Model VI. Metal dynamics in subsequent years are then computed by first speciating
168 the total geochemically active metal into adsorbed and dissolved pools, then calculating the
169 change in the geochemically active pool, and the annual leaching flux, according to Equation
170 (1).

2.3. Catchments, soils and atmospheric deposition

172 The locations of the catchments from which soils were sampled are shown in Figure 1. The
173 catchments comprise the following:

174   1. Four small sub-catchments (0.3–1.8 km^2 in area) of the upper River Duddon in the
175   English Lake District. The catchments are Gaitscale Gill (GG), Troughton Gill (TG),
176   Hardknott Gill (HKG) and Castle How Beck (CHB). The landscape is high relief with
177   altitude within the catchments varying from 200–800 metres above sea level (m.a.s.l.).
178   Vegetation is predominantly grassland, with appreciable areas of bare rock (20% of
179   the total area). Soils at higher altitude are largely thin humic rankers, with some peats,
180   with areas of humic brown earth soils towards valley bottoms.

181 2. The catchment of Scoat Tarn (ST) (0.8 km^2), a small mountain lake in the western
182   Lake District. General catchment and soil characteristics are similar to those for the
183   upper Duddon; catchment altitude varies from 600–820 m.a.s.l..

184 3. An area of 0.4 km^2 on the western side of Great Dun Fell (GDF), in the Pennine hills
185   of central northern England. The area is shallow–sloped, at an altitude of
186   approximately 500 m.a.s.l., and comprises peat and ranker soils. The vegetation is
187   heather–grass moorland and wetland. Precipitation is around 1300 mm a^{-1}.

188 4. The River Etherow (RE) and Howden Reservoir (HR) catchments, in the southern
189   part of the Pennines range. These are neighbouring catchments with areas of 13 km^2
190   and 36 km^2, and altitudes of 310–630 m.a.s.l. and 290–600 m.a.s.l., respectively. Soils
191   and vegetation in both catchments are similar; soils comprise peats and podzols and
192   the vegetation is largely heather moorland with some areas of rough grazing.

193 5. Lochnagar (LN) is a mountain catchment in the eastern part of the Cairngorms massif
194   in the Scottish Highlands, at an altitude of 790–1150 m.a.s.l. and an area of 1.2 km^2.
195   The catchment comprises heather-grass moorland with peaty soils and an extensive
196   proportion (50%) of bare rock, and a corrie lake of area 0.1 km^2.

197 6. The Old Lodge (OL) catchment is situated in Ashdown Forest in south east England.
198   The catchment has an area of 0.4 km^2 and comprises lowland heathland with some
199   improved grassland and a small portion of woodland. Soils are cambisols and podzols.
200   Catchment altitude varies from 105–190 m.a.s.l..

201 The approach to soil sampling has been previously been described by Tipping et al. (2006a;
202 2006b; 2010). Briefly, soils were sampled in five or six locations in each catchment by
203 digging pits to the maximum accessible depth, i.e. to bedrock or to large stones. In peaty
204 catchments (GDF, RE and HR), soils were sampled to a depth of 10cm in wetter places and
205 to 20cm in drier places. Separate soil samples were taken from organic and mineral horizons
206 where both were encountered. Soil pH, C content, concentrations of geochemically–active
207 metals and bulk densities were measured. Soil pH was determined on supernatants obtained
208 by extraction of soil with 1 mM NaCl at a field moist soil:solution ratio of 1:2.5. Soil carbon
209 was determined by elemental analysis (Universal CHNS-O Vario EL elemental analyser).
210 Geochemically–active soil metal concentrations were determined following extraction with
211 0.1M HNO$_3$. Contents of trace elements and Si in representative rock samples were
212 determined by X–ray fluorescence (British Geological Survey).

213 The collection and processing of bulk atmospheric deposition has been described previously
214 (Lawlor and Tipping, 2003; Tipping et al., 2007; Yang et al., 2002). Deposition was collected
215 in the Duddon, GDF, RE and OL catchments using polypropylene funnels and polyethylene
216 collection vessels and analysed by ICP–MS, and in the LN catchment using an RS-1 type
217 precipitation collector. Sample collection and processing followed strict cleanliness
218 protocols. Trace metal determination was done by ICP–MS.

219 **3. Model application**

220 *3.1. Timespan of simulations*

221 The objective of this study was to predict present day pools of metals in the topsoils of the
222 study catchments from measurements and estimates of historic metal deposition. To do this,
223 we assumed that the soil metal pools were in steady state with deposition and weathering in
224 the year 1400, as was previously done by Tipping et al. (2006b) and Tipping et al. (2010).
225 Simulations were started from this date and run to 2010.

226 *3.2. Atmospheric deposition*

227 The overall shape of the time trend in atmospheric deposition of metals to was derived from
228 the observations of Ochsenbein et al. (1983) on metal concentrations in sediments cores from
229 Blelham Tarn in the English Lake District. Deposition was assumed to comprise a constant
230 background rate D_B, a variable rate D_A due to deposition of metal emitted at regional and
231 national scale, and a second variable rate due to deposition of metal emitted due to mining
232 and smelting activities in the local region of the catchment $D_{A,\,local}$. The deposition profile
233 started in 1400 with a rate equal to D_B. Regional/national scale anthropogenic deposition was
234 assumed to start in a year y_0 (1600 for Pb, 1800 for the other metals) and to increase over
235 time to 1960 according to the expression

236
$$D_A = D_{A,\,max}\left(\frac{y - y_0}{1960 - y_0}\right)^n \tag{4}$$

237 where D_A is the deposition rate (g ha^{-1} a^{-1}), y is the year for which deposition is being
238 calculated, y_0 is the starting year, $D_{A,\,max}$ is the deposition in 1960 and n is a constant. From
239 1960 to 1970 anthropogenic deposition was assumed to be constant at a rate of $D_{A,\,max}$, after
240 which it declines linearly to 2000 and then remains constant to 2010.

241   Deposition profiles were first calculated for the Duddon catchments (GG, TG, HKG and

242   CHB) and scaled to the measured present–day deposition fluxes in the GDF, RE and OL

243   catchments. Deposition fluxes at ST were assumed to be equal to those in the Duddon

244   catchments, and those at HR assumed to be equal to those in the RE catchment. In both cases

245   this assumption was based on the proximity of the catchments to each other. Deposition

246   profiles for LN were derived by adjustment of the parameters of Equation 4 to observed

247   metal profiles in the sediments of the lake within the catchment (Tipping et al., 2007).

248   The possible influence of additional local metal deposition ($D_{A, local}$), due to mining activities,

249   was investigated in the RE and HR catchments. To incorporate historic local deposition we

250   used the time series profiles constructed by Tipping et al. (2010), which represent idealised

251   scenarios. Local deposition was assumed to start in 1700, increase linearly until 1830 to a

252   value $D_{A, local, max}$, then remain constant until 1860 and decrease linearly to zero in 1900. For

253   these catchments, scenarios were run both including and omitting the local deposition.

254   Parameter values for Equation 4 are given in Table S1.

3.3. Soil properties

256   We derived for each catchment a single idealised soil profile representing the 'best average'

257   physicochemical properties (pH, soil organic matter content, bulk density, stony material

258   content) of the sampled catchment soils. This was done using the same approach previously

259   used by Tipping et al. (2006a) and Tipping et al. (2010) based on surveys of soils across each

260   catchment, but deriving a single 'best average' set of properties for the complete soil layer,

261   rather than for two layers. The properties derived are listed in Table S2.

262   Pools of 'geochemically active' metal, expressed on an areal basis (mol m^{-2}), were calculated

263   for each sampling location within the catchment from soil metal concentrations,bulk density

264   and the proportion of stony material, as previously described in detail by Tipping et al.

265   (2006b) and Tipping et al. (2010). Mean values for each catchment are given in Table S3.

3.4. Metal weathering

267   We used the weathering rates of metals into the soil pool (F_{weath}) (mol m^{-2} a^{-1}) previously

268   calculated by Tipping et al. (2006b) and Tipping et al. (2010). These calculations assumed

269   that metals are weathered by congruent dissolution of silicate minerals. Weathering rates

270   were calculated from the streamwater flux of Si and the metal:Si ratios in minerals.

271   Weathering rates for each catchment are given in Table S4.

3.5. Porewater pH, DOC and SPM concentrations

Modelling with the IDMM requires time series data for soil pH, as the model does not itself compute this variable. Where historic changes in soil pH are known or suspected to have occurred in the catchment, reconstruction or estimation of a time trend for model input may be appropriate. The catchments simulated here have all been subject to historic anthropogenic acidification, with more recent evidence for declines in acidification (Tipping et al., 2000; Davies et al., 2005). Past trends in pH may be estimated by a number of methods, such as from diatom assemblages preserved in lake sediments (e.g. Birks et al., 1990), or by simulation using an acidification model such as MAGIC (Cosby et al., 1985). For the simulations presented here, we used time series of soil porewater pH predicted by the CHUM-AM model (Tipping et al., 2006a, 2007, 2010; Ashmore et al., 2007) as inputs. The porewater pH in the CHUM-AM simulations was calculated for two soil layers, which for the IDMM runs have been bulked to form a single mixed layer. A single porewater pH for this layer was calculated from the CHUM-AM predictions by taking the mean of the predicted pHs for each year, weighted for the soil solid mass in each of the layers used for the CHUM-AM simulations. The time trends in porewater pH are shown for each catchment in Figure 2. It can be seen that soil acidification is predicted to begin between 1600 and 1700 and to increase in rate in the 1800s to reach a minimum pH around 1960-1980, after which a partial recovery towards pristine values is predicted to occur. Concentrations of DOC and SPM in the porewater were set equal to the concentrations in drainage from the lowest soil horizon in the CHUM-AM simulations (Tipping et al., 2006b, 2010). The influence of erosion on the predicted soil metal pools was assessed by also performing model with the porewater SPM concentration set to zero.

3.6. Metal soil-solution partitioning

The distribution of metal between the free ion in porewater and the geochemically active pool (Equation (2)) was calculated using one of two sets of parameters. The first was derived by Shotbolt and Ashmore (2004) using a dataset derived from UK soils. The dataset comprised chemical analyses of (i) 95 upland grassland topsoils of England and Wales (Tipping et al., 2003) (Cu, Zn, Cd and Pb only), (ii) 56 topsoils from locations with mixed land uses (deciduous woodland, heathland, upland coniferous forest, acid grasslands and lowland coniferous forest), and (iii) 16 topsoils, comprising soils from three locations contaminated by historic Pb mining, and three neighbouring uncontaminated locations. The methods

304 described by Tipping et al. (2003) were used for the extraction of soil porewaters and
305 chemical analysis of soils and porewaters. The geochemically active soil metal pools were
306 estimated by extraction with 0.1M sodium EDTA at a soil:solution ratio (w:v) of 1:10. Free
307 metal ion concentrations in the porewater were calculated using WHAM/Model VI (Tipping,
308 1998). We will refer to the transfer functions derived using these data as set A.

309 In order to make a comparison with a transfer function parameterised on a wider range of soil
310 types, we also performed model runs using the transfer function parameters calculated for
311 Equation (2) by Groenenberg et al. (2010), which we will refer to as set B. These parameters
312 were calculated from three datasets: the UK non-forested upland soils dataset already
313 described, and two datasets comprising measurements from soil samples of the Netherlands.
314 The Groenenberg et al. datasets cover a slightly smaller range of porewater pH (3.3–8.3) and
315 a wider range of soil organic matter content (0.5%–97.8%) compared to the UK–only
316 datasets (pH 3.0–8.3 and soil organic matter 4.6%-97.8%). Parameter values for both sets of
317 transfer functions are provided in Table 1.

318 Comparisons of the predictions made by each set of transfer functions are shown in Figure
319 S1. The figure illustrates how the predicted free metal ion concentrations change with
320 increasing soil organic matter content, for two porewater pH values, and a single
321 geochemically active metal concentration. For Ni, transfer function B predicts higher free ion
322 concentrations, indicating weaker binding to the soil. The difference between the predictions
323 is smaller at higher pH and lower soil organic matter content; at a soil pH of 6 and an organic
324 matter content of 10% or lower, the predictions are similar. Copper is predicted to have a
325 difference dependence of binding strength on soil organic matter content. At a soil organic
326 matter content of 50%, predicted binding strengths are very similar, while at lower soil
327 organic matter transfer function A predicts stronger binding and at higher soil organic matter
328 transfer function B predicts stronger binding. Conversely, the predictions for Zn show that
329 both transfer functions predict similar dependences of binding strength on soil organic matter
330 content, but show different dependences on pH: at a porewater pH of 3 transfer function A
331 predicts stronger binding, while at pH 6 transfer function B predicts stronger binding. The
332 predictions for Cd are very similar, while for Pb transfer function A consistently predicts
333 stronger binding. This is particularly pronounced at low soil organic matter contents ($\leq$10%),
334 where the free ion predicted by transfer function A is over an order of magnitude lower than
335 that predicted using transfer function B.

11

336   *3.7. Dynamic model application*

337   Model runs were performed for the period 1400 to 2010, assuming that in 1400 the soils were

338   in steady state with respect to their chemistry and organic matter content. The model was

339   initially applied to each catchment without optimisation of parameters. For the catchments

340   where only regional deposition was considered, two simulations were made, one with each

341   transfer function. For the catchments where both local and regional deposition were

342   considered, four runs were made, considering regional deposition only, and considering

343   regional and local deposition, using each transfer function.

344   Model performance was assessed by comparing the observed and predicted soil pools for

345   each metal for the year for which observations were available. Temporal trends were also

346   assessed to consider the predicted metal behaviour.

347   **4. Results**

348   *4.1. Time series predictions*

349   Examples of time series predictions for two catchments, TG and HR, are shown in Figure 3.

350   Nickel, Zn and Cd are all predicted to show reductions in soil pools in response to lower

351   deposition inputs since 1970, while Cu and Pb show reduced accumulation but no net losses.

352   *4.2. Predicted retention of metals by catchment soils*

353   Retention of anthropogenic metal by the soils to 1970 and 2000 is shown in Figure S2. The

354   metals show contrasting patterns of retention. Generally, retention increases in the order

355    $Zn < Ni < Cd < Cu < Pb$ in simulations using transfer function A. In simulations using

356   transfer function B, the order is similar with the exception that Ni shows slightly lower mean

357   retention than Zn. Copper retention is higher in simulations using transfer function B (mean

358   81%) than in simulations using transfer function A, while the opposite trend is seen for Pb,

359   with mean 93% retention in simulations using transfer function set A and 83% in simulations

360   using transfer function set B. Nickel, Zn and Cd generally show greater cross–catchment

361   variability in retention than do Cu and Pb.

362   Simulated changes in soil metal pools in response to reduced deposition from 1970 to 2000

363   also show patterns dependent on the metal and the transfer function used for simulation.

364   Generally, Cu and Pb are predicted to continue accumulating in most catchments,

365   independent of the transfer function used. Cd is predicted to have continued to accumulate in

12

366 around half the catchments and to have shown a net loss in the remainder, while both Ni and

367 Zn are predicted to have shown net losses in most of the catchments.

368 Examination of the role of soil erosion on metal loss showed that for Ni, Cd and Zn,

369 predicted metal losses in erosion at the present day were consistently less than 5% of the total

370 losses, regardless of catchment or transfer function used. Erosional losses of copper were also

371 consistently below 5% with the exception of HR where they were predicted to be 7% when

372 using transfer function A and 9% when using transfer function B. Erosional losses of Pb were

373 predicted to comprise a widely proportion of the total losses, across all the catchments. When

374 using transfer function A, proportional losses were predicted to range from 0.5% for RE to

375 34% for HR and 47% for GDF. When using transfer function B, losses ranged from less than

376 0.1% for OL to 8% for HR and 26% for GDF.

377 The influence of simulating erosion on the prediction of soil metal pools was variable. When

378 erosion was not simulated, present–day metal pools were consistently predicted to be higher

379 than in the simulations where erosion was simulated. For Ni, Zn and Cd, the difference in

380 present–day pools was less than 0.1% in all the catchments except GDF and HR, regardless

381 of the transfer function used. For Cu and Pb, the differences covered a wider range. For Cu,

382 the largest difference seen was 1.5%, in the GDF catchment, with transfer function A, and

383 3.3%, in HR, with transfer function B. For Pb, the respective largest differences were 14.3%

384 (HKG) and 5.5% (GDF). The largest differences for Ni, Zn and Cd respectively were 2.3%,

385 0.9% and 2.1% using transfer function set A, and 1.3%, 0.8% and 1.9% using transfer

386 function set B. All these differences were observed in the GDF catchment.

387 *4.3. Influence of local deposition*

388 Figure 4 illustrates the effect of simulating additional local metal deposition on the

389 predictions of metal pools in the HR catchment. In all cases the addition of local deposition,

390 with an earlier onset date than the regional deposition, results in higher metal pools at an

391 earlier date. In the cases of Ni, Zn and Cd, the model predicts that present day pools would be

392 very similar to those seen if there were no additional deposition, with pools in the presence of

393 local deposition calculated to be 1.1, 1.0 and 1.1 times higher, respectively, than the pools

394 predicted in the absence of local deposition. In the cases of Cu and Pb, local deposition is

395 predicted to have a residual effect on current day pools. For Cu the pool is predicted to be 1.8

396 times larger than in the absence of local deposition, while the Pb pool is predicted to be 2.0

397 times larger. The proportional predicted increases in present day metal pools for the three

13

398 catchments for which scenarios including local deposition have been run are shown in Figure

399 S3. Generally, the addition of local deposition has the largest influence on the predicted Pb

400 pools, with a near doubling of the present day pools predicted. Conversely, present day pools

401 of Zn are predicted to be little affected by the addition of local deposition.

402 *4.4.   Comparison with observed soil metal pools*

403 Figure 5 compares observed present day metal pools in all the catchment with IDMM

404 predictions using transfer function set A, and Figure 6 shows the equivalent comparison for

405 transfer function set B. The model predicts the observed present day Zn and Cd pools to

406 within a factor of three in all the catchments and the observed Cu and Pb to within the same

407 degree in nine catchments. Nickel pools are predicted to the same degree in seven of the

408 catchments. Overall, the root mean squared differences in the (logged) observed pools, for

409 Ni, Cu, Zn, Cd and Pb respectively, are 0.40, 0.35, 0.24, 0.29 and 0.39 when using transfer

410 function set A. When using transfer function set B, Zn and Cd pools are predicted to within a

411 factor of three in nine and eight catchments respectively, and Cu and Pb pools to within the

412 same degree in seven catchments. Nickel is predicted to within the same degree in all ten

413 catchments. The root mean squared differences for Ni, Cu, Zn, Cd and Pb are 0.33, 0.43,

414 0.27, 0.31 and 0.46 respectively.

415 The predicted soil pools of Pb exhibit some distinctive patterns compared to the observed

416 pool. The observed present day pool in the RE catchment soils (100 mmol m^{-2}) is over seven

417 times greater than the pool predicted by the IDMM using either transfer function (13.1 mmol

418 m^{-2} using transfer function set A and 8.61 mmol m^{-2} using transfer function set B). This pool

419 is also greater than the sum of the total anthropogenic input of Pb and the predicted steady

420 state pool under pristine conditions, when using either transfer function. In two catchments

421 (LN and OL) the model predicts that the present day pool would be overestimated by the

422 model even in the absence of any anthropogenic deposition, when using transfer function set

423 A (Figure S4). Conversely, this is not observed in either catchment when using transfer

424 function set B, and the model achieves good agreement between observation and prediction.

425 Clear trends towards over– or under–prediction of observed metal pools were noted for Ni,

426 Cu, Cd and Pb, when using either transfer function. In the case of Pb, as already noted, this

427 may result from overestimation of the pristine pool or apparent underestimation of the

428 anthropogenic inputs. In the case of the other metals, uncertainties in the transfer functions

429 are a plausible source of this bias. To investigate this we optimised the constant term α_0 in the

14

430   transfer functions for Ni, Cu, Zn and Cd to achieve the best fit between (logged) observed

431   and predicted metal pools. For transfer function set A, optimal fits (Figure 5) were obtained

432   by adjusting α_0 by -0.27, -0.33, 0.15 and 0.38 respectively, resulting in root mean squared

433   deviations of 0.29, 0.29, 0.18 and 0.12. For transfer function set B, optimal fits (Figure 6)

434   were obtained by adjusting α_0 by 0.12, -0.43, 0.15 and 0.41 respectively, resulting in root

435   mean squared deviations of 0.30, 0.30, 0.22 and 0.13.

436   **5.   Discussion**

437   The IDMM generally makes reasonable predictions of present day metal pools in the

438   catchments studied here, given the inherent uncertainty in the historic metal deposition

439   profiles and the within-catchment variability in soil properties and metal pools. Also, despite

440   the relatively simple nature of the model compared to CHUM-AM, which we have previously

441   applied to these catchments (Tipping et al., 2006; 2010), the model predicts reasonably

442   similar soil pools (Figure S5). Thus, the IDMM has clear promise as a model for predicting

443   the dynamics of metals in soils on the basis of relatively simple inputs.

444   The IDMM describes the solid-solution partitioning of metals by coupling an empirical

445   transfer function with a chemical speciation model for the computation of porewater metal

446   speciation. This is a somewhat more complex approach than is often taken in chemical fate

447   models where a simple partition coefficient (K_d) approach is used to compute the distribution

448   of chemical between solid and dissolved (i.e. porewater) phases. Such an approach has also

449   been shown to provide a good description of soil–solution partitioning for metals, where the

450   dependence of K_d upon soil and porewater properties is modelled (e.g. Groenenberg et al.,

451   2012), and could readily be incorporated into the IDMM. The reason for adopting the more

452   complex, 'coupled' approach it allows calculation of the free metal ion concentration. Since

453   the free ion concentration is a key variable in metal uptake and toxicity models, this

454   potentially allows the IDMM to be coupled to models such as the terrestrial BLM (Thakali et

455   al., 2006), the free ion approach (Lofts et al., 2004; Lofts et al., 2013) and Freundlich–based

456   uptake modelling approaches (e.g. Plette et al, 1999; Mertens et al., 2007) Thus, the

457   simplicity of a K_d–based approach is sacrificed to allow greater model potential, without the

458   need to take a purely mechanistic approach.

459   The comparison of transfer functions suggested that transfer function set A in general

460   performed better than transfer function set B, despite being derived from a smaller set of soils

461   with a narrower range of physicochemical properties. However, set A simulated Pb relatively

462   poorly in two catchments (OL and LN), due to overestimating the steady state soil pool. The

463   porewater Pb concentration at steady state is calculated so that Pb losses in leaching balance

464   the inputs, therefore it is independent of the transfer function. Since set A predicts greater

465   binding of Pb to the soil than does set B, this must necessarily result in a higher steady state

466   adsorbed pool. Clearly, the performance of both transfer functions for Pb suggests that the set

467   B parameters are providing the more realistic estimates of metal distribution between free ion

468   and soil–adsorbed forms,

469   A useful development would be to use soil data to calibrate the model directly, by optimising

470   the transfer function coefficients, instead of relying on values determined from soil

471   experiments. This could provide tighter relationships between prediction and observation, and

472   thereby more precise predictions. Adjustment of the constant term in the transfer function, as

473   we have done in this study, is a useful alternative method, despite being less satisfactory

474   since it makes the assumption that all bias is due to a single parameter.

475   Extension of the model to other trace metals and metalloids is clearly possible, given suitable

476   parameterisation. Metals that exist in cationic form are clearly amenable to incorporation, if

477   transfer function parameters and solution complexation constants, including binding to DOC,

478   become available. Anionic metals and metalloids, such as molybdenum and arsenic, present

479   distinct, although not insurmountable issues. The binding characteristics of these species to

480   dissolved organic matter are poorly known compared to the metals simulated in this study,

481   and so more fundamental DOM–binding studies and model development would be required

482   before such species could be incorporated into the IDMM at the same level of complexity. A

483   first step would be to express soil–solution partitioning of such species as a single empirical

484   function, as has been done, for example, by Groenenberg et al. (2012) for Mo and As. This

485   would alleviate the need to explicitly consider binding to DOM as a separate process, but

486   would be potentially less useful for linking to toxicity modelling since it would not entail

487   calculation of the free ion concentrations.

488   The role of soil erosion as a present day loss process was predicted in most cases to be

489   relatively minor in comparison to losses as dissolved metal in soil drainage, and to have a

490   minor influence on the prediction of present day metal pools in the topsoils. An exception

491   was Pb, where differences in predictions with and without erosion occasionally exceeded

492   10%.Applications of the model to other soils are clearly desirable. Its ease of application

493   means that it can be tested for many sites, using generic histories of metal deposition (and

494   acidification if relevant), but taking into account local variations where known. Thus, in

16

principle the IDMM could be applied to sufficient representative soils to permit national assessments of soil metal dynamics, including future scenarios. In particular, there is potential scope for application to other soil systems apart from the ones described here, such as agricultural systems receiving metal inputs from sources such as sludges, manures and fertilisers. Another possible improvement would be to add a second soil box, so that the slow downward movement of metals through soil could be represented. This would also open the possibility of incorporating a description of metal transfer to surface waters and groundwaters, permitting integrated assessment of metal dynamics in a similar manner to CHUM-AM. Wider application of the model could benefit from more detailed consideration of processes causing metal losses, particularly erosion, which may be significantly higher in lowland catchments (e.g. Chambers et al., 2000; Chapman et al., 2005). Additionally, the selective erosion of particles enriched in metals relative to the bulk soil (e.g. Quinton and Catt, 2007) could be usefully incorporated into the model.The IDMM provides a suitable framework within which to test the influence of processes not currently considered in heavy metal dynamic models. For example, it could be used to assess the influence of metal storage, cycling and removal in biomass (e.g. trees in forested catchments, crops in arable catchments), and the effects of fixation ("ageing") processes whereby metal added to soil in geochemically active form is rendered unreactive by incorporation into mineral matter. Existing models of metal fixation (e.g. Crout et al., 2006) could readily be incorporated into the IDMM.

6. Conclusions

The Intermediate Dynamic Model for Metals (IDMM) provides generally reasonable predictions of present day metal (Ni, Cu, Zn, Cd, Pb) pools in a series of semi-natural UK catchments, based on profiles of historic metal deposition and soil pH. Agreement between observation and prediction can generally be improved by optimising the transfer functions describing the partitioning of metal between the free ion and the soil-bound pool. In the case of Pb, the generally strong predicted retention in the soil makes the historic deposition rate the most important driving variable in the predictions. The IDMM provides a potentially useful tool for large scale application to study and predict topsoil metal dynamics. Additional processes such as metal fixation and biomass uptake could be readily incorporated in order to simulate more complex systems than those studied here.

References

Ashmore, M., Van den Berg, L., Terry, A., Tipping, E., Lawlor, A.J., Lofts, S., Thacker, S.A., Vincent, C.D., Hall, J., O'Hanlon, S., Shotbolt, L., Harmens, H., Lloyd, A., Norris, D., Nemitz, E., Jarvis, K., Jordan, C., 2007. Development of an Effects-based Approach for Toxic Metals. Report to the UK Department for Environment, Food and Rural Affairs, the Scottish Executive, the National Assembly for Wales and the Department of the Environment in Northern Ireland. Contract CPEA 24. University of York.

Bhavsar, S.P., Gandhi, N., Diamond, M.L., 2008. Extension of coupled multispecies metal transport and speciation (TRANSPEC) model to soil. Chemosphere 70, 914–924.

Birks, H.J.B., Line, J.M., Juggins, S., Stevenson, A.C., Terbraak, C.J.F., 1990. Diatoms and pH reconstruction. Philosophical Transactions of the Royal Society B-Biological Sciences 327, 263–278.

Bonten, L.T.C., Groenenberg, J.E., Meesenburg, H., de Vries, W., 2011. Using advanced surface complexation models for modelling soil chemistry under forests: Solling forest, Germany. Environmental Pollution 159, 2831–2839.

Chambers, B.J., Garwood, T.W.D., Unwin, R.J., 2000. Controlling soil water erosion and phosphorus losses from arable land in England and wales. Journal of Environmental Quality 29, 145–150.

Chapman, A.S., Foster, I.D.L., Less, J.A., Hodgkinson, R.A., 2005. Sediment delivery from agricultural land to rivers via subsurface drainage. Hydrological Processes 19, 2875–2897.

Cosby, B. J., Hornberger, G. M., Galloway, J. N. & Wright, R. F., 1985. Modelling the effects of acid deposition: assessment of a lumped parameter model of soil water and stream chemistry. Water Resources Research, 21, 51–63.

555   Crout, N.M.J., Tye, A.M., Zhang, H., McGrath, S.P., Young, S.D., 2006. Kinetics of metal

556   fixation in soils: Measurement and modeling by isotopic dilution. Environmental Toxicology

557   and Chemistry 25, 659–663.

558   Davies, J.J.L., Jenkins, A., Monteith, D.T., Evans, C.D., Cooper, D.M., 2005. Trends in

559   surface water chemistry of acidified UK Freshwaters, 1988–2002. Environmental Pollution

560   137, 27–39.

561   de Vries, W., Groenenberg, J.E., 2009. Evaluation of approaches to calculate critical metal

562   loads for forest ecosystems. Environmental Pollution 157, 3422–3432.

563   Groenenberg, J.E., Römkens, P.F.A.M., Comans, R.N.J., Luster, J., Pampura, T., Shotbolt,

564   L., Tipping, E., de Vries, W., 2010. Transfer functions for solid-solution partitioning of

565   cadmium, copper, nickel, lead and zinc in soils: derivation of relationships for free metal ion

566   activities and validation with independent data. European Journal of Soil Science 61, 58–73.

567   Groenenberg, J.E., Dijkstra, J.J., Bonten, L.T.C., de Vries, W., Comans, R.N.J., 2012.

568   Evaluation of the performance and limitations of empirical partition–relations and process–

569   based multisurface models to predict trace element solubility in soils. Environmental

570   Pollution 166, 98–107.

571   Hall, J.R., Ashmore, M., Fawehinmi, J., Jordan, C., Lofts, S., Shotbolt, L., Spurgeon, D.J.,

572   Svendsen, C., Tipping, E., 2006. Developing a critical load approach for national risk

573   assessments of atmospheric metal deposition. Environmental Toxicology and Chemistry 25,

574   883–890.

575   Lawlor, A.J., Tipping, E., 2003. Metals in bulk deposition and surface waters at two upland

576   locations in northern England. Environmental Pollution 121, 153–167.

577   Lofts, S., Spurgeon, D.J., Svendsen, C., Tipping, E., 2004. Deriving soil critical limits for Cu,

578   Zn, Cd, and Pb: A method based on free ion concentrations. Environmental Science and

579   Technology 38, 3623–3631.

580   Lofts, S., Chapman, P., Dwyer, R., McLaughlin, M., Schoeters, I., Sheppard, S., Adams, W.,

581   Alloway, B., Antunes, P., Campbell, P., Davies, B., Degryse, F., de Vries, W., Farley, K.J.,

582   Garrett, R.G., Green, A., Groenenberg, B.J., Hale, B., Harrass, M., Hendershot, W.H., Keller,

583   A., Lanno, R., Liang, T., Liu, W.-X., Ma, Y., Menzie, C., Moolenaar, S.W., Piatkiewicz, W.,

584   Reimann, C., Rieuwerts, J.S., Santore, R.C., Sauvé, S., Schuetze, G., Schlekat, C., Skeaff, J.,

585   Smolders, E., Tao, S., Wilkins, J., Zhao, F.-J., 2007. Critical loads of metals and other trace
586   elements to terrestrial environments. Environmental Science & Technology 41, 6326–6331.

587   Lofts, S., Tipping, E., Hamilton-Taylor, J., 2008. The Chemical Speciation of Fe(III) in
588   Freshwaters. Aquatic Geochemistry 14, 337–358.

589   Lofts, S., Criel, P., Janssen, C.R., Lock, K., McGrath, S.P., Oorts, K., Rooney, C.P.,
590   Smolders, E., Spurgeon, D.J., Svendsen, C., van Eeckhout, H., Zhao, F.–J., 2013. Modelling
591   the effects of copper on soil organisms and processes using the free ion approach: towards a
592   multi-species toxicity model. Environmental Pollution 178, 244–253.

593   Mertens, J., Degryse, F., Springael, D., Smolders, E., 2007. Zinc toxicity to nitrification in
594   soil and soilless culture can be predicted with the same biotic ligand model. Environmental
595   Science and Technology 41, 2992–2997.

596   Ochsenbein, U., Davison, W., Hilton, J., Haworth, E.Y., 1983. The geochemical record of
597   major cations and trace metals in a productive lake. Archiv für Hydrobiologie 98, 463–488.

598   Paces, T., 1998. Critical loads of trace metals in soils: A method of calculation. Water, Air
599   and Soil Pollution, 105, 451–458.

600   Plette, A.C.C., Nederlof, M.M., Temminghoff, E.J.M., van Riemsdijk, W.H., 1999.
601   Bioavailability of heavy metals in terrestrial and aquatic systems: A quantitative approach.
602   Environment Toxicology and Chemistry 18, 1882–1890.

603   Posch, M., de Vries, W., 2009. Dynamic modelling of metals – Time scales and target loads.
604   Environmental Modelling & Software 24, 86–95.

605   Quinton, J.N., Catt, J.A., 2007. Enrichment of heavy metals in sediment resulting from soil
606   erosion on agricultural fields. Environmental Science and Technology 41, 3495–3500.

607   Shotbolt, L., Ashmore, M.R., 2004. Extension of Critical Loads Mapping to Forests and
608   Lowland Vegetation: Derivation of New Transfer Functions. Annexes to the Final Report to
609   Defra EPG 1/3/188. Defra, London, pp. 137–163.

610   Thakali, S., Allen, H.E., Di Toro, D.M., Ponizovsky, A.A., Rooney, C.P., Zhao, F.J.,
611   McGrath, S.P., 2006. A Terrestrial Biotic Ligand Model. 1. Development and application to
612   Cu and Ni toxicities to barley root elongation in soils. Environmental Science and
613   Technology 40, 7085–7093.Tipping, E., 1995. CHUM: a hydrochemical model for upland
614   catchments. Journal of Hydrology 174, 305–330.

615 Tipping, E., 1996. CHUM: a hydrochemical model for upland catchments. Journal of
616 Hydrology 174, 305–330.

617 Tipping, E., 1998. Humic Ion-Binding Model VI: an improved description of the interactions
618 of protons and metal ions with humic substances. Aquatic Geochemistry 4, 3–48.

619 Tipping, E., 2005. Modelling Al competition for heavy metal binding by dissolved organic
620 matter in soil and surface waters of acid and neutral pH. Geoderma 177, 293–304.

621 Tipping, E., Bettney, R., Hurley, M.A., Isgren, F., James, J.B., Lawlor, A.J., Lofts, S., Rigg,
622 E., Simon, B.M., Smith, E.J., Woof, C., 2000. Reversal of acidification in tributaries of the
623 River Duddon (English Lake District) between 1970 and 1998. Environmental Pollution 109,
624 183–191.

625 Tipping, E., Rieuwerts, J., Pan, G., Ashmore, M.R., Lofts, S., Hill, M.T.R., Farago, M.E.,
626 Thornton, I., 2003. The solid-solution partitioning of heavy metals (Cu, Zn, Cd, Pb) in
627 uplands soils of England and Wales. Environmental Pollution 125, 213–225.

628 Tipping, E., Lawlor, A.J., Lofts, S., 2006a. Simulating the long-term chemistry of an upland
629 UK catchment: Major solutes and acidification. Environmental Pollution 141, 151–166.

630 Tipping, E., Lawlor, A.J., Lofts, S., Shotbolt, L., 2006b. Simulating the long-term chemistry
631 of an upland UK catchment: Heavy metals. Environmental Pollution 141, 139–150.

632 Tipping, E., Yang, H., Lawlor, A.J., Rose, N.L., Shotbolt, L., 2007. Trace metals in the
633 catchment, loch and sediments of Lochnagar: Measurements and modelling. In: Rose, N.L.
634 (Ed.), Lochnagar: The Natural History of a Mountain Lake. Developments in
635 Paleoenvironmental Research, vol. 12. Springer, Dordrecht, The Netherlands, pp. 345–370.

636 Tipping, E., Rothwell, J.J., Shotbolt, L., Lawlor, A.J., 2010. Dynamic modelling of
637 atmospherically-deposited Ni, Cu, Zn, Cd and Pb in Pennine catchments (northern England).
638 Environmental Pollution 158, 1521–1529.

639 Yang, H., Rose, N.L., Batterbee, R.W., 2002. Distribution of some trace metals in Lochnagar,
640 a Scottish mountain lake ecosystem and its catchment. The Science of the Total Environment
641 285, 197–208.

642   Table 1. Derived parameters for transfer functions A and B.

	Transfer function A			
	α_0	α_1	α_2	N
Ni	-4.84	0.31	0.93	0.70
Cu	-5.17	1.17	0.78	1.00
Zn	-3.28	0.36	0.90	1.00
Cd	-5.85	0.39	0.95	0.68
Pb	-4.20	1.12	0.72	1.00
	Transfer function B			
	α_0	α_1	α_2	N
Ni	-4.76	0.45	0.91	0.84
Cu	-6.37	0.64	0.87	0.57
Zn	-4.67	0.46	0.84	0.84
Cd	-5.71	0.41	0.91	0.70
Pb	-6.46	0.96	1.35	0.84

643

644

Figures

Figure 1. Locations of modelled catchments. A = Lochnagar; B = Great Dun Fell (GDF); C = Scoat Tarn; D = Upper Duddon (Gaitscale Gill, Troughton Gill, Hardknott Gill, Castle How Beck); E = River Etherow; F = Howden Reservoir; G = Old Lodge.

Figure 2. Time trends in soil porewater pH, predicted by the CHUM-AM model and used as inputs to the IDMM simulations. Catchment abbreviations are as follows: HKG = Hardknott Gill; CHB = Castle How Beck; TG = Troughton Gill; GG = Gaitscale Gill; GDF = Great Dun Fell; HR = Howden Reservoir; BER = Blackstone Edge Reservoir; RE = River Etherow; OL = Old Lodge; LN = Lochnagar.

Figure 3. Time trends of geochemically active metal concentrations (mol m^{-2}) in TG catchment soils (left hand plots) and HR catchment soils (right hand plots). Points represent individual determinations of geochemically active metal pools. Lines represent IDMM simulations. Thin solid lines: simulations using transfer function set A; thin dashed lines: simulations made transfer function set B.

Figure 4. Time trends of geochemically active metal concentrations (mol m^{-2}) in HR catchment soils, with and without the consideration of local deposition and using transfer function set A. Points represent individual determinations of geochemically active metal pools. Lines represent IDMM simulations. Thin solid lines: including national/regional deposition only; dashed lines: simulations including national/regional and local deposition. All simulations use the UK soils transfer function.

Figure 5. Comparison between mean observed and simulated soil metal pools (mmol m^{-2}) when using transfer function set A. Solid points represent blind predictions, open points represent fits obtained by optimisation of the constant term in the transfer function.

Figure 6. Comparison between mean observed and simulated soil metal pools (mmol m^{-2}) when using transfer function set B. Solid points represent blind predictions, open points represent fits obtained by optimisation of the constant term in the transfer function.
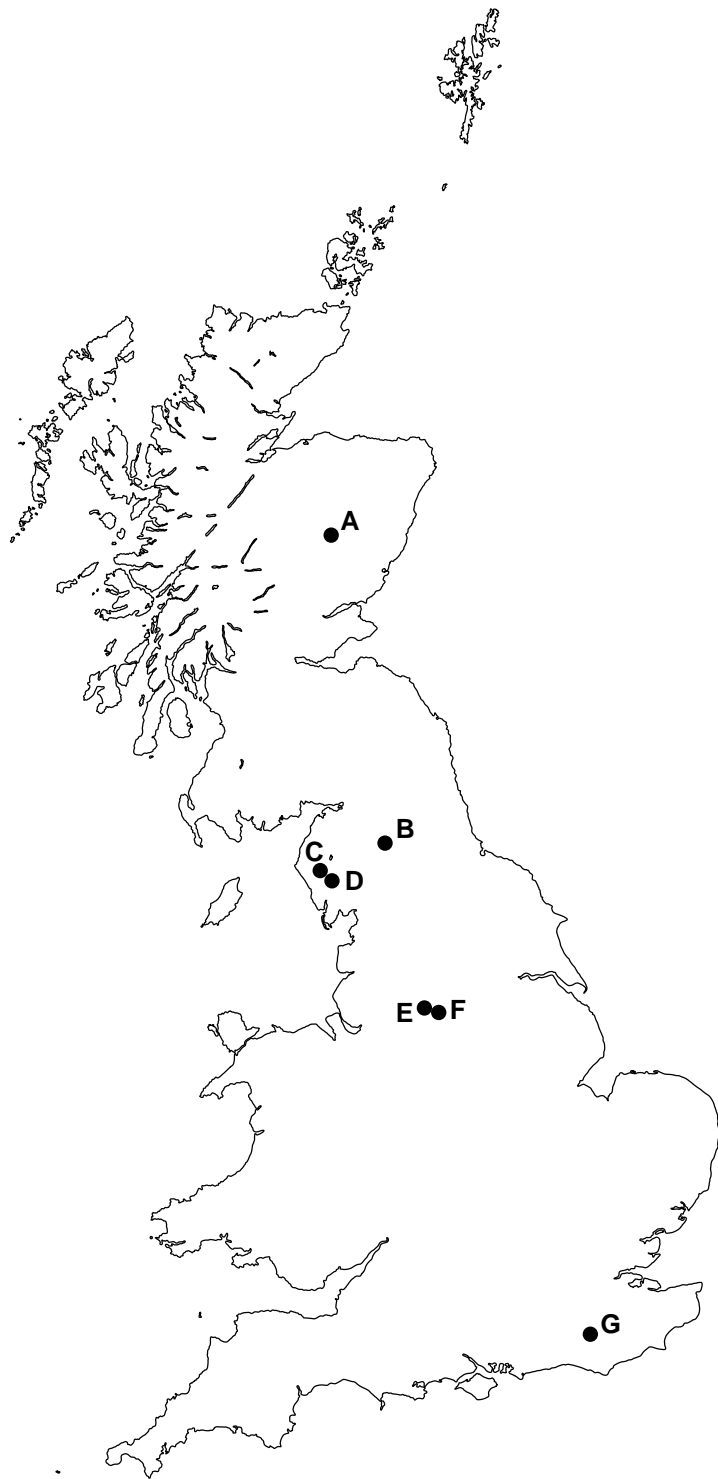
672

673   Figure 1.

674
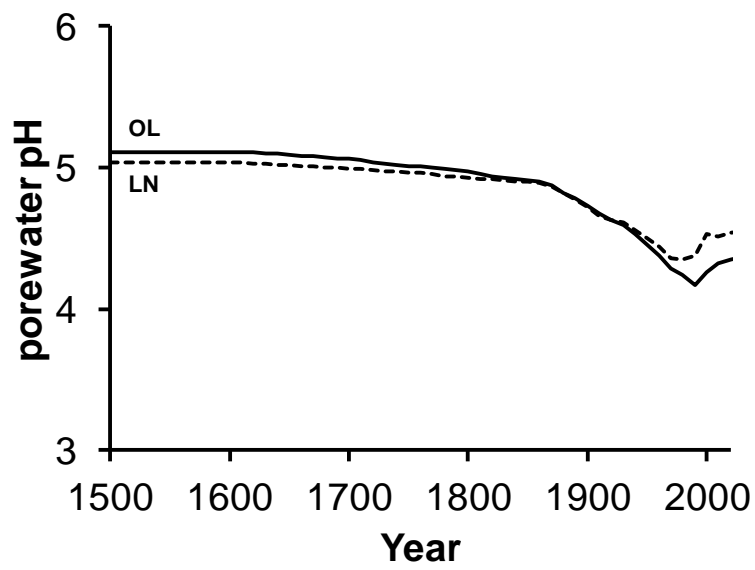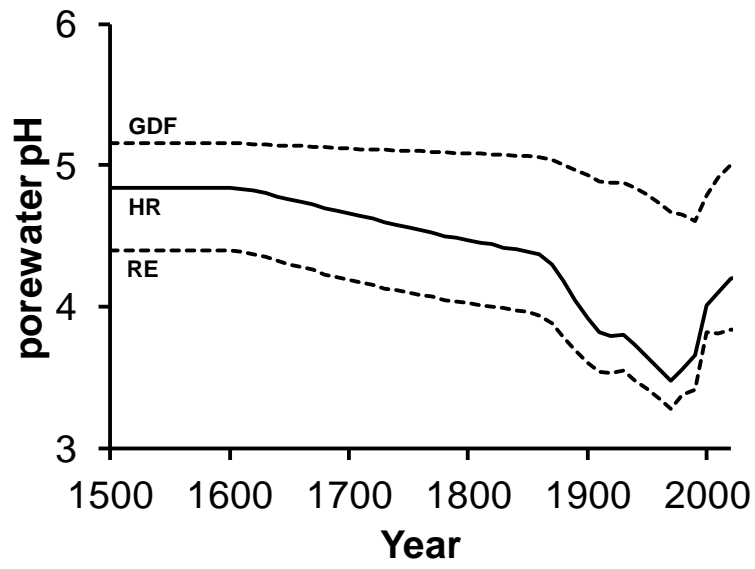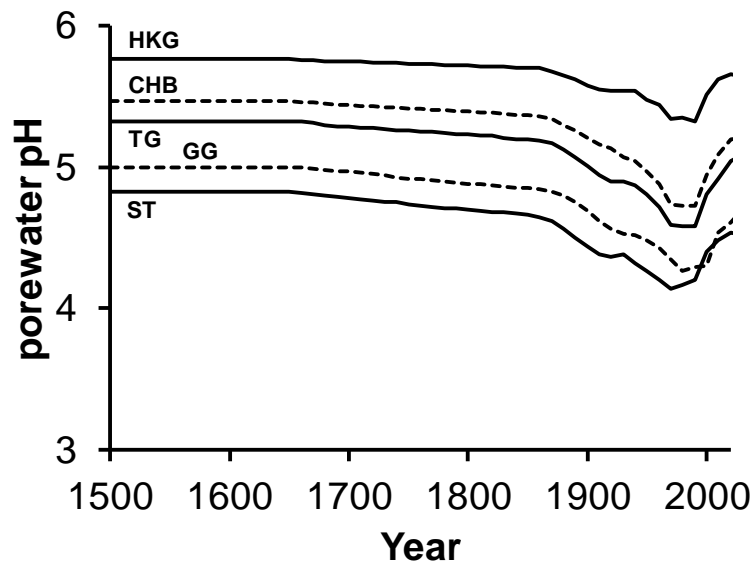
675

676 Figure 2.

677

678   Figure 3.

26

679
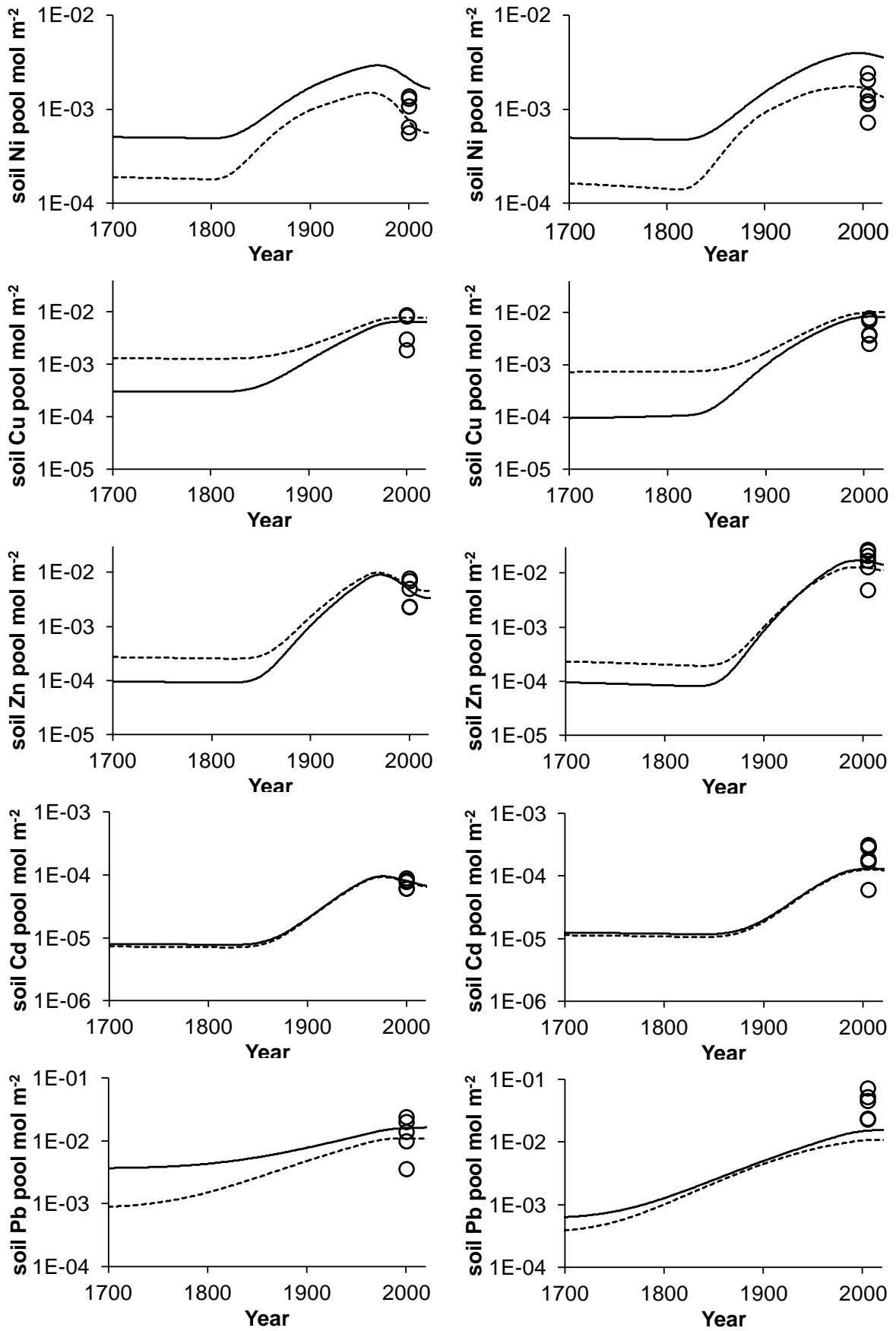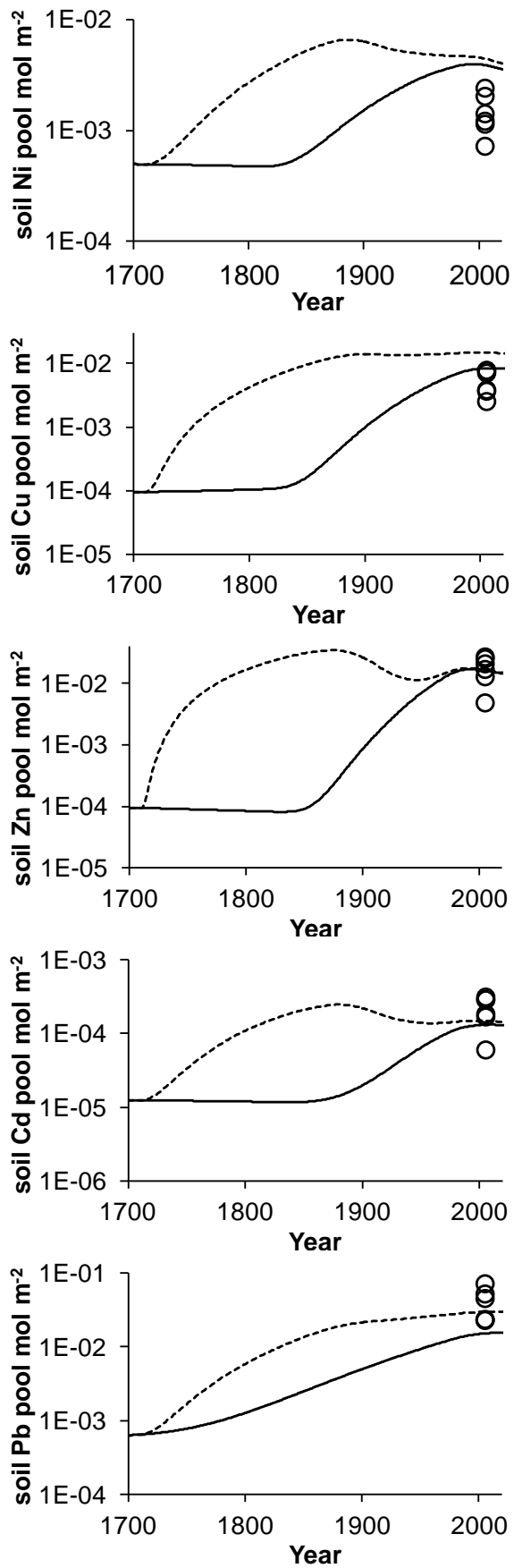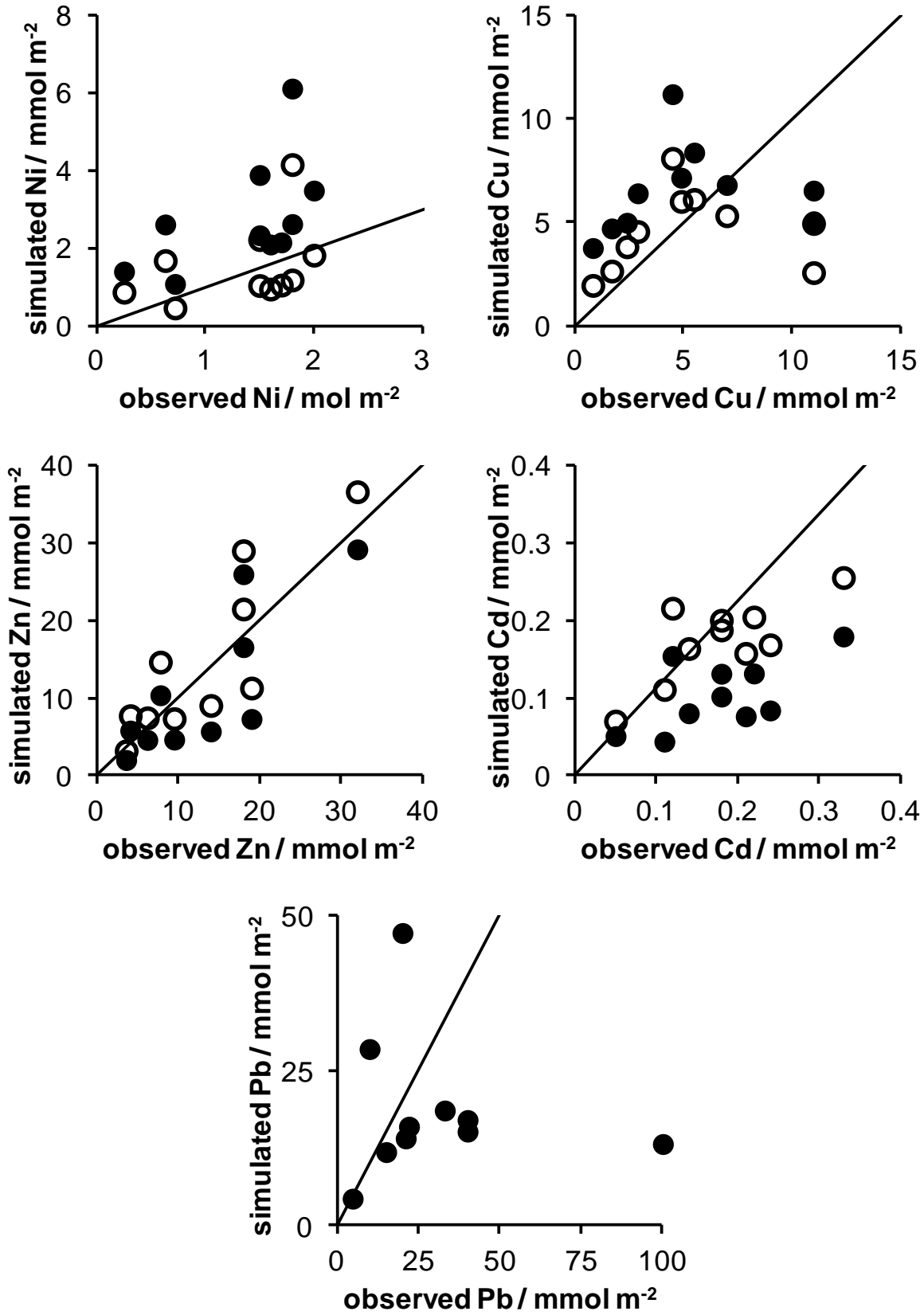
Figure 4.

681

682   Figure 5.

683

684

685   Figure 6.

686